CrossMark

Effect of the Outer Diameter on the Behavior of Square RC Columns Strengthened with Self-Compacting Concrete Filled Circular Steel Tube

Yiyan Lu[1] · Zhenzhen Liu[1] · Shan Li[1] · Xiaobo Zhao[1]

Abstract

This paper aimed to investigate the optimum outer diameter of square RC columns strengthened with self-compacting concrete filled circular steel tube. An experiment of twelve strengthened RC columns (SRC) and two referential RC columns subjected to axial load was presented. The variables considered in the test were the confinement index and the diameter of the strengthened section. The experimental results showed that, with the same confinement index, the material strength utilization of SRC columns dropped with the increasing of strengthened section diameter. There existed an optimum outer diameter to take full use of material strength. With the outer diameter below the optimum value, the material strength utilization increased with increasing confinement index. As the outer diameter beyond the optimum one, the material strength utilization decreased with improving confinement index.

Keywords RC columns · Strengthening method · Self-compacting concrete (SCC) · Concrete filled steel tube (CFST) · Optimum outer diameter · Confinement index · Material strength utilization

1 Introduction

Global structural failures and progressive collapse mostly originate from the failure of critical structural elements such as column, slab and shear wall (Crawford et al. 1997; Gilmour and Virdi 1988). To avoid the catastrophic consequences, it is crucial to improve the reliability of the critical structural elements, which is reduced by design errors, construction deviation, change of structure usage, aging of structure itself and upgrading to confirm to current code requirements (Abdel-Hay and Fawzy 2015; Iqbal et al. 2016). Reinforcement concrete (RC) column, as the most important structural element, is usually strengthened by many common techniques including concrete jacketing (Colomb et al. 2008; Vandoros and Dritsos 2008), FRP confinement (Bonacci and Maalej 2001; Nanni and Norris 1995; Pellegrino and Modena 2002; Sheikh and Yau 2002) and steel jacketing (Aboutaha et al. 1999; Abedi et al. 2010) to improve its reliability. Meanwhile, more new strengthening techniques are still carried out continuously, among

that the method of using concrete filled steel tube (CFST) to strengthen RC columns is drawing increasing interest of researchers.

CFST columns, combining the advantages of concrete jacketing and the desirable mechanical performance of itself, have the potential to be used in strengthening RC columns. CFST columns, consisting of a steel tube filled with concrete, combine the beneficial qualities of steel and concrete materials (Han 2007; Xiong et al. 2017; Zhong 2003). Steel tube acts as a confining jacket and non-corrosive reinforcement for the concrete core, thereby improving concrete strength (Chitawadagi et al. 2012; Dundu 2012; Uy et al. 2011). Concurrently, the concrete core prevents or delays local buckling of the steel tube and carries load in compression (Elremaily and Azizinamini 2002; Gupta et al. 2007; Giakoumelis and Lam 2003). This combination results in the improved strength, stiffness, and ductility over the sum of the individual components (Yu et al. 2008; Han et al. Han 2008). Furthermore, construction time and cost can be saved by the stay-in-place structural formwork (Kyung et al. 2008; Liu et al. 2015). The strengthening method of CFST takes those advantages to improve the performance of RC columns. The strengthening procedure is to strip off the protective layer and deficient section of RC columns firstly, then pack the steel tube welded by two pieces of L-shaped

✉ Shan Li
  lishan@whu.edu.cn

1 School of Civil Engineering, Wuhan University,
   Wuhan 430072, China

or semicircular steel plates, and pour into concrete lastly to make them work together. Then an effective confinement will be obtained from the steel tube to the concrete core, which puts the concrete under a triaxial state of stress and causes a significant increase in concrete strength. The filled concrete simultaneously prevents the steel tube from buckling inward. Consequently, both ultimate capacity and ductility of the RC column will be significantly increased with small cross-section changes.

There are some literatures available about the method of using CFST to strengthen RC columns. Priestley et al. (1994a, b) firstly proposed the strengthening method of CFST and investigated the mechanical behavior of the strengthened RC columns. The results indicated that lateral stiffness and ductility of RC columns were remarkably improved. Then this strengthening method had been used in the field of strengthening bridge pier columns. Xiao (2003) used the partially stiffened steel jackets to strengthen RC columns. It was reported that this strengthening method not only prevented brittle shear failure but also substantially improved the ductility of RC columns. Sezen and Miller (2011) compared the effectiveness of various strengthening methods, including concrete jacketing, FRP-composite wrap and CFST jacketing. Comparisons indicated that the strengthening effect of CFST jacketing was more evident than the others. Xu and Cai (2007) reported a series of experimental research on RC columns strengthened by circular steel jacketing subjected to axial or eccentric loading. The test results demonstrated the effectiveness of using CFST to strengthen RC columns in terms of bearing capacity and ductility. Wang (2011) presented an experimental study on the axial behavior of RC columns strengthened by circular steel tube with initial stress. By strengthening, the load-bearing capacity of RC columns was improved as well as the ductility. The increase of initial load had little effect on the loading-bearing capacities, while it can affect the ductility to some extent. Zhou et al. (2012) described an axial load test about six circular RC columns strengthened by CFST. The confinement of steel tube on concrete core was proved to be more obvious with the increase of steel tube thickness, which is in favour of the strengthening effect.

However, the gap between the formwork (steel tubes) and RC columns is so narrow to vibrate concrete that the formwork cannot be filled uniformly by normal vibrated concrete. Consequently, many defects exist on the concrete surface due to the imperfect compaction. The satisfactory results of the CFST strengthening method is seriously affected by the defects. To deal with this puzzle, Lu et al. (2015a, b, c) innovatively proposed to use self-compacting concrete (SCC) instead of normal vibrated concrete to fill in steel tubes. SCC has the high fluidity to reach to parts of the formwork with gravity instead of vibration and completely fill the mold cavity to form a uniform dense concrete, which is a guarantee of the strengthening

effect (Holschemacher 2004; Muciaccia et al. 2011; Patrick et al. 2005). Lu et al. (2015a, b, c) has investigated the behavior of RC columns strengthened with SCC filled steel tubes subjected to axial or eccentric load. The column section types included circular RC columns strengthened with circular CFST and square RC columns strengthened with square CFST. The information about the behavior of square RC columns strengthened with SCC filled circular steel tubes is still scarce. Meanwhile, the former researches focused on investigating the influence of wall thickness of the steel tube, designed strength grade of strengthening concrete, initial eccentricity and length-to-width ratio. But comparatively limited research was carried out to investigate the optimum outer diameter of the strengthened section.

Therefore, this paper performs an experimental investigation on the effect of the outer diameter on the behavior of square RC columns strengthened with SCC filled circular steel tubes. This research is conduced to take full use of the material strength. The variables considered in the test are the confinement index and the diameter of the strengthened section. The failure mode, the ultimate capacity, the axial shortening behavior and the ductility of SRC columns are investigated.

2 Experimental Program

2.1 Test Specimens

A total of fourteen square RC columns were tested under axial load, including two columns without strengthening, to be used as control references. The other twelve columns were strengthened with SCC filled circular steel tubes. The RC columns had a 150×150 mm^2 square cross section and an overall height of 800 mm. Four deformed bars with 12 mm nominal diameter were used as longitudinal reinforcement in RC columns. The transverse reinforcement consisted of stirrups with 6 mm nominal diameter.

The strengthening procedure was divided into four steps: (1) Roughened the concrete surface of RC column with steel brush; (2) packed the RC column into the steel tube jacket welded by two pieces of semicircular steel plates; (3) poured SCC into the spare between RC column and steel tube; (4) cured the concrete in nature until 28 day age. The strengthening procedure and the cross section details of specimens are shown in Fig. 1.

Details of the specimens are summarized in Table 1. The considered parameters are the diameter of the strengthened section and the confinement index (CI). In this study, the confinement index (CI) is defined as:

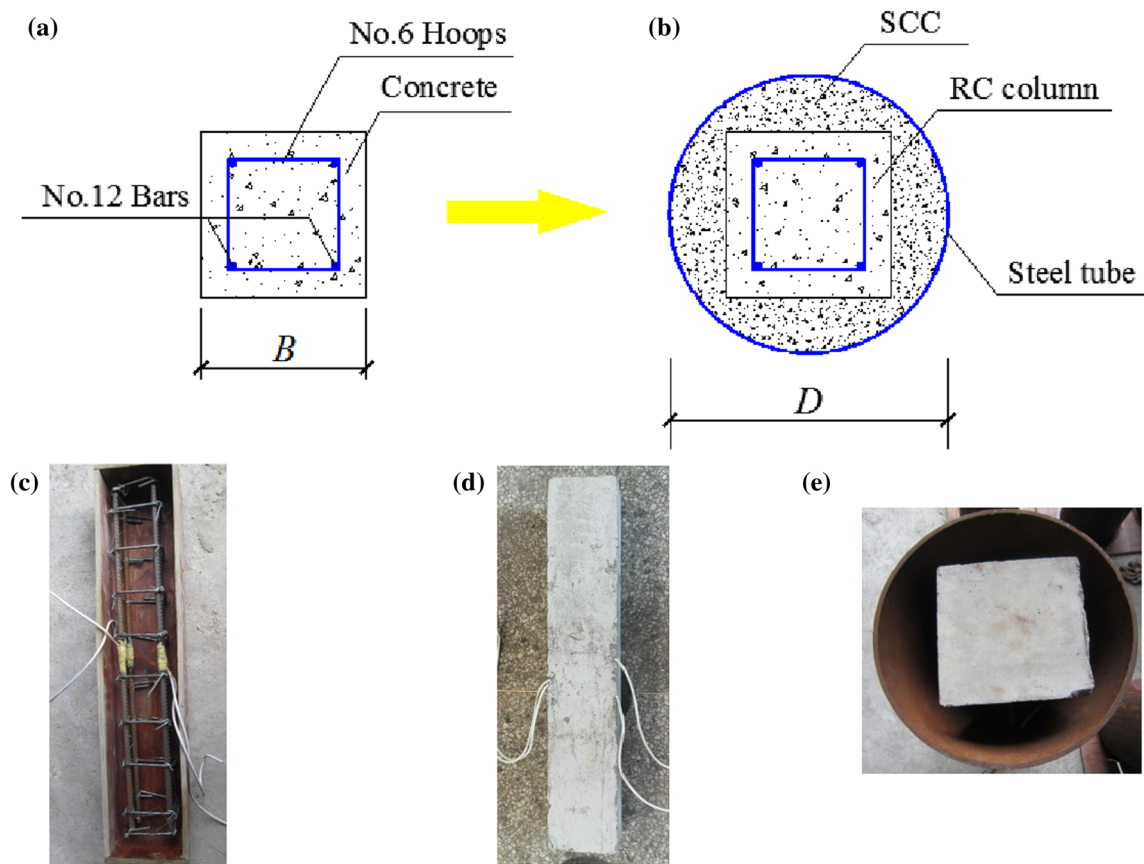$$CI = \frac{A_s f_{sy}}{A_{c1} f_{c1} + A_{c2} f_{c2}} \tag{1}$$

Fig. 1 The strengthening procedure of specimens: **a** cross section of RC column; **b** cross section of strengthened column; **c** assembling rebar of RC column; **d** manufactured RC column; **e** pack the RC column with steel tube

Table 1 Details of the specimens

Group	Specimen ID	$D(B) \times t$ (mm)	$f_{cu,m1}$ (MPa)	$f_{cu,m2}$ (MPa)	θ	CI	SI	DI	N_{exp} (kN)
RC columns	RC1	150×0	31.52	–	–	–	–	1.34	714
	RC2	150×0	31.52	–	–	–	–	1.30	702
SRC-D1	SRC-D1-t1.5	250×1.76	31.52	44.87	3.52	0.42	1.282	1.52	2491
	SRC-D1-t2.5	250×2.76	31.52	44.87	3.92	0.61	1.287	2.08	2778
	SRC-D1-t3.5	250×3.58	31.52	44.87	4.27	0.80	1.288	2.59	3024
SRC-D2	SRC-D2-t1.5	273×1.76	31.52	44.87	4.09	0.36	1.275	1.51	2893
	SRC-D2-t2.0	273×2.10	31.52	44.87	4.17	0.43	1.260	1.54	2951
	SRC-D2-t2.5	273×2.76	31.52	44.87	4.46	0.54	1.248	1.84	3156
	SRC-D2-t3.0	273×3.16	31.52	44.87	4.59	0.62	1.240	2.14	3252
	SRC-D2-t3.5	273×3.58	31.52	44.87	4.78	0.71	1.247	2.53	3385
	SRC-D2-t4.0	273×4.14	31.52	44.87	4.89	0.81	1.216	3.20	3465
SRC-D3	SRC-D3-t1.5	300×1.76	31.52	44.87	4.86	0.32	1.283	1.48	3444
	SRC-D3-t2.5	300×2.76	31.52	44.87	5.30	0.48	1.274	1.63	3751
	SRC-D3-t3.5	300×3.58	31.52	44.87	5.52	0.62	1.230	2.43	3905

where A_{c1} and A_{c2} are the cross-sectional areas of the original concrete and strengthening concrete, respectively. f_{sy} is the yield strength of the steel tube, f_{c1} and f_{c2} are the axial compressive strengths of the original concrete and strengthening concrete, respectively. The strengthened section diameter was designed as 250 mm, 273 mm and

Table 2 Concrete mixes

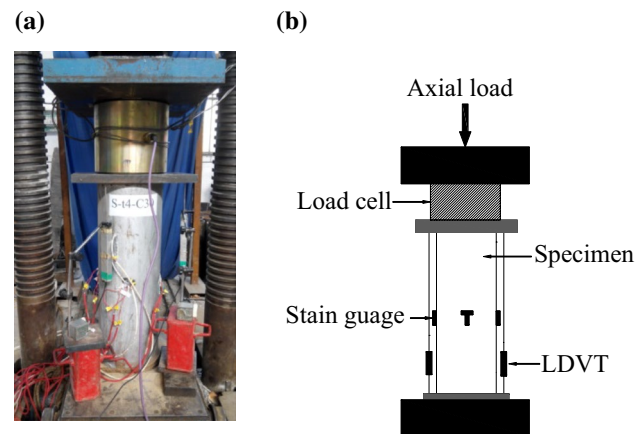| Concrete ID	Mix proportion by weight	Slump flow (mm)	f_{cu} (MPa)
	Cement: gravel: sand: water: fly ash: water reducer: expansive agent		
C25	1.000:4.082:2.103:0.635:0.000:0.000:0.000	–	31.52
C40	1.000:2.390:2.240:0.510:0.430:0.014:0.002	270	44.87

Table 3 Material properties of steel

Steel	t or D (mm)	f_y (MPa)	Elongation (%)	E_s (GPa)
Steel tube	1.76	366	24.6	205
	2.10	369	25.4	191
	2.76	346	23.2	209
	3.16	350	27.6	211
	3.58	343	23.8	215
	4.14	340	22.0	234
Stirrup	6.00	310	25.0	189
Longitudinal reinforcement	12.00	458	21.9	195

Fig. 2 Test arrangement: **a** photograph; **b** diagrammatic view

300 mm. Different confinement indexes (*CI*) were achieved by changing the thickness of tube. For convenience, each strengthened specimen had an individual designation as: SRC-DY-tX, where X is the nominal wall thickness of steel tube in mm and Y stands for the different diameters of the strengthened section.

2.2 Material Properties

In order to simulate a column with low compressive strength in need of strengthening, the concrete strength grade of RC columns was designed as 25 MPa. According to the Chinese code GB 50367-2013 (2013), the strength grade of strengthening concrete should be higher than the original concrete and 30 MPa. Therefore, the strength of SCC was designed as 40 MPa. The mix designs for original and strengthening concrete are shown in Table 2. Three concrete cubes with dimension of $150 \times 150 \times 150$ mm³ were cast at the same time of concrete pouring. The mean compressive cube strengths at 28 day age and the slump flow of SCC are also shown in Table 2.

Six kinds of nominal thickness of tube (1.5, 2, 2.5, 3, 3.5 and 4 mm) were used in the test. Standard tensile coupon tests, according to Chinese codes GB/T 2975-1998 (1998), were conducted to measure material properties of the steel tube and rebars. The mean actual thicknesses (*t*), the average yield strengths (*f*y), the modulus of elasticity (*E*s) and elongation of steel are summarized in Table 3.

2.3 Test Setup

All the specimens were tested under a computer monitored hydraulic jack with capacity of 5000 kN. Figure 2 gives the details of test setup and instrument layout. The specimens were applied the axial load through the flat hinge. A force transducer was placed above the top of flat hinge to accurately measure the applied load in time. Two linear variable differential transducers (LVDTs) were vertically located to measure the axial deformation of specimens. Four strain gauges were attached on the four longitudinal rebars and eight strain gauges were symmetrically attached around the surface of steel tube at the mid-span. The arrangement of strain gauges is exhibited in Fig. 3. All the specimens were loaded in small increments of 1/10 ultimate bearing capacity in the elastic stage and 1/15 ultimate bearing capacity after the steel yield. The tests stopped when the load dropped to 85% of ultimate load.

3 Test Results and Discussions

3.1 Failure Mode and Test Observation

The RC columns without strengthening failed by the crushing of concrete and the buckling of the longitudinal rebars as shown in Fig. 4. The first significantly wide cracking of concrete was observed when the applied load reach to 80%

Fig. 3 The arrangement of strain gauges
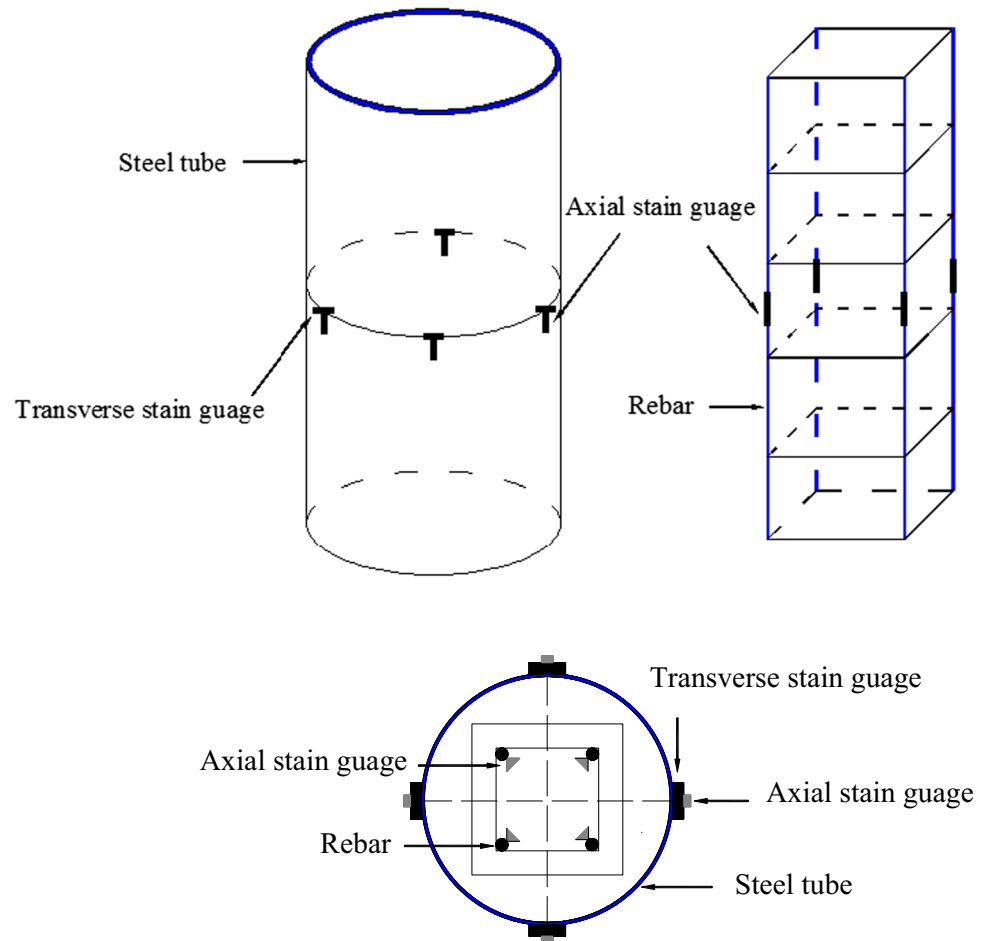
of the maximum load. As the load increases, the number and width of concrete crack developed. As approaching to the end of test, the concrete was spalling and the longitudinal rebars were obviously buckling.

As presented in Figs. 5, 6, 7, two types of failure modes were exhibited in the SRC columns: shear failure and local buckling failure. An initial linear elastic behavior was observed for all columns. When the applied load reach to 60–70% of the maximum load, the shear line appeared on the steel tubes of eight SRC columns. With the increasing of load, the shear line became more obvious as depicted in Fig. 5. After the test, in order to have a better visualization of the concrete core failure mode, the external steel tube was cut and removed. It was observed that a diagonal penetrating crack emerged in the strengthening concrete. Then striping off the strengthening concrete, the failure mode of RC columns was similar to the strengthening concrete.

With the greatest *CI*, the specimen SRC-D2-t4.0 and SRC-D1-t3.5 experienced local buckling failure as shown in Fig. 6. The bulge was initiated at the middle part of the column when the imposed load reached to 60–70% of the ultimate load. With a further increase of the imposed load, the bulge was more apparent. When the ultimate load was

approached, local buckling near the top and bottom surface of column was observed. After the external steel tube was removed, the strengthening concrete was found to crush at the location of outward folding of steel tube and no shear failure plane was observed. Striping off the strengthening concrete, the similar failure mode was exhibited. This phenomenon can be due to the effective confinement provided by steel tube.

Only the specimen SRC-D3-t1.5 exhibited seam weld failure near the bottom surface of steel tube as seen in Fig. 7. The seam weld failure occurred at the loading of 80% of the ultimate load and developed towards the middle part of steel tube with the increasing load. After the test, striping off the steel tube, both the strengthening concrete and original concrete crushed at the location of seam weld failure.

3.2 Axial Load-Axial Shortening Curve

Plots of axial load versus axial shortening for all specimens are given in Figs. 8, 9, 10. The axial shortening is the average value of two LVDTs. All the curves present the similar shape: an ascending branch is followed by a descending branch. Initially, the axial load increases as the axial

Fig. 4 Typical failure of RC columns without strengthening

shortening increases linearly until the load is up to approximately 60–80% of the ultimate load. Then the curve deviates from its initial linearity and the axial load increases much more slowly until a peak value. At the softening stage, the

axial load drops gradually to about 85% of the maximum loading ($0.85\,N_u$).

Figure 8 compares the behavior of RC columns and SRC columns. The SRC columns have a longer linear stage and go into nonlinear stage at about 80% of the ultimate load. However, the curves of the RC columns exhibit nonlinearity when the load reaches to 60% of the ultimate load. Meanwhile, the slope of SRC columns in linear stage is deeper, indicating a higher stiffness. The corresponding axial shortening at 85% of the ultimate load for the SRC columns is higher than that of RC columns, showing an increased ductility. Based on the analysis above, SRC columns have a superior performance to RC columns in terms of ultimate capacity, rigidity and ductility.

Figure 9 illustrates the effect of the strengthened section diameter on axial shortening respond of SRC columns. With the similar confinement index (*CI*), the specimen with larger diameter of the strengthened section exhibits a longer and deeper linear stage. It means that the rigidity increases as the diameter of the strengthened section increases. On the other hand, the ultimate strength increases with the improvement of the strengthened section diameter.

Figure 10 presents the comparison of the behavior of SRC columns with various confinement indexes (*CI*). The specimens with a higher *CI*-value have a longer linear stage. It can be explained that the more remarkable confinement effect improves the concrete strength and lengthens the elastic stage of specimen. In the softening stage, the axial load of SRC columns with higher *CI*-value drops more slowly. It can be seen that the specimens with the larger *CI* not only have a longer linear stage but also an improved ductility.

3.3 Ultimate Capacity

The ultimate capacity during test is defined as the maximum load of the axial load versus shortening curve. The ultimate capacities of specimens are listed in Table 1. It is clear that the

Fig. 5 Shear failure of SRC columns: **a** steel tube; **b** strengthening concrete; **c** RC column
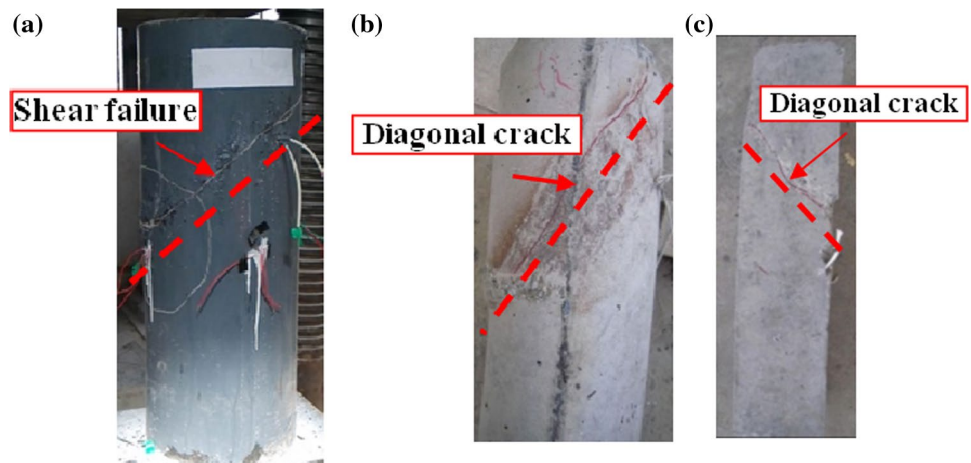
Fig. 6 Local buckling failure of SRC columns: **a** steel tube; **b** strengthening concrete; **c** RC column
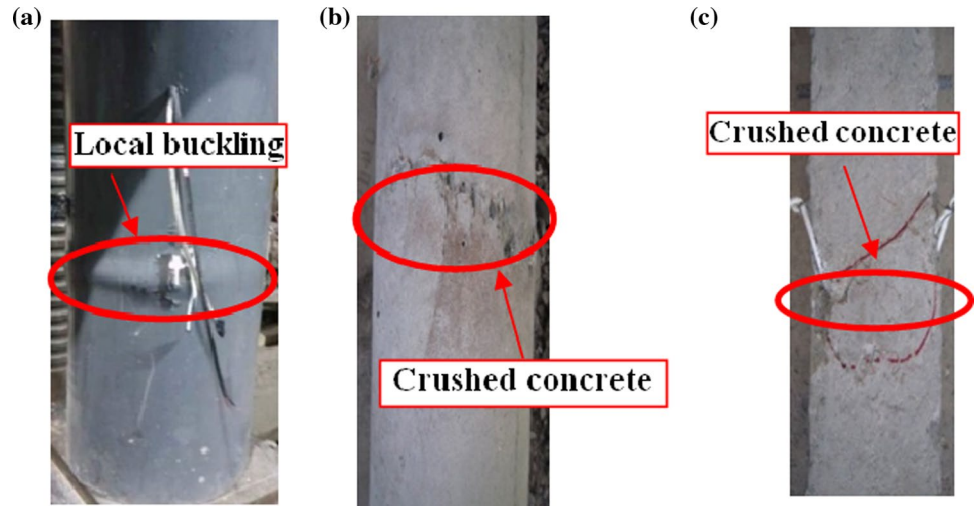

Fig. 7 Seam weld failure of SRC columns: **a** steel tube; **b** strengthening concrete; **c** RC column
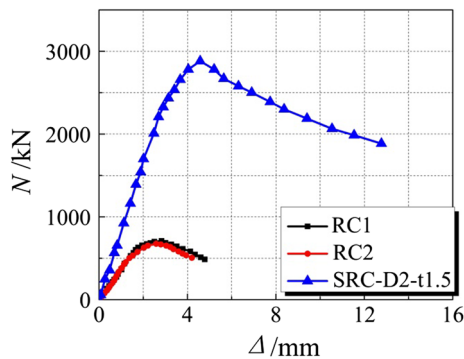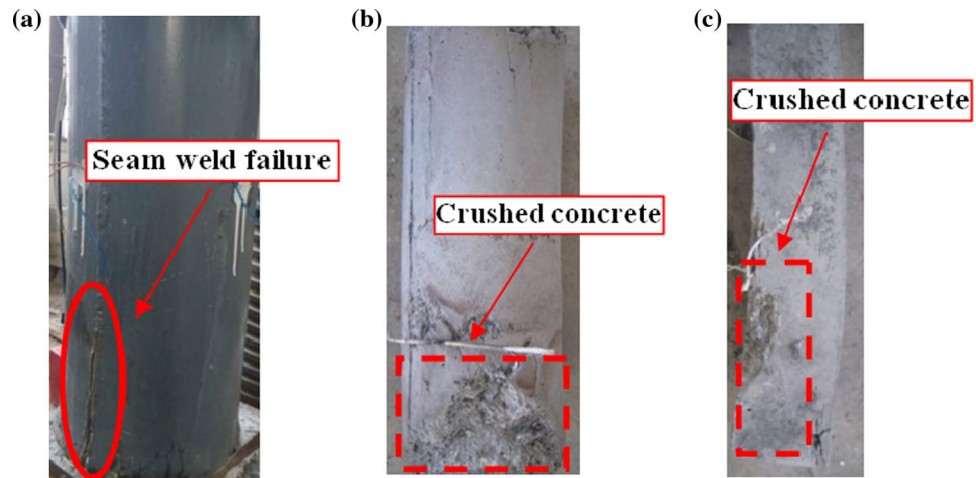

Fig. 8 Comparison of load-axial shortening curve between RC columns and SRC columns

strengthening method has a significant impact on the ultimate capacity. In order to evaluate the efficiency of this strengthening method, an enhancement ratio θ is introduced and defined as:

$$\theta = \frac{N_{SRC}}{N_{RC}} \tag{2}$$

where N_{RC} and N_{SRC} are the ultimate capacities of RC columns and SRC columns, respectively. N_{RC} is the average value of the ultimate capacities of two referential RC columns.

The values of enhancement ratio are presented in Fig. 11. The enhancement ratio ranges between 3.52 and 5.52, and the mean ratio is 4.53, indicating the effectiveness of this strengthening method. The influence trend of the strengthened section diameter and CI is as expected: the enhancement ratio increases with the increasing of the strengthened section diameter or CI. It is worth noting that CI has a more distinct influence on the enhancement ratio than the strengthened section diameter.
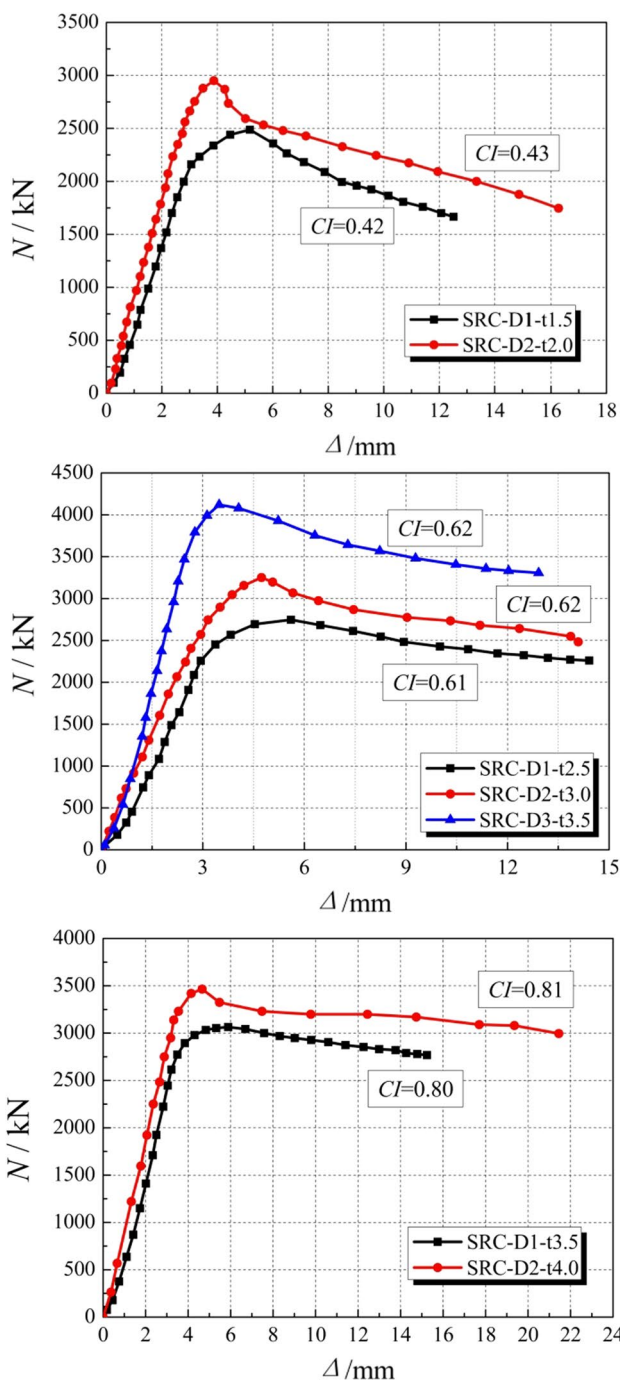
Fig. 9 Axial load-axial shortening curves with various diameters of the strengthened section
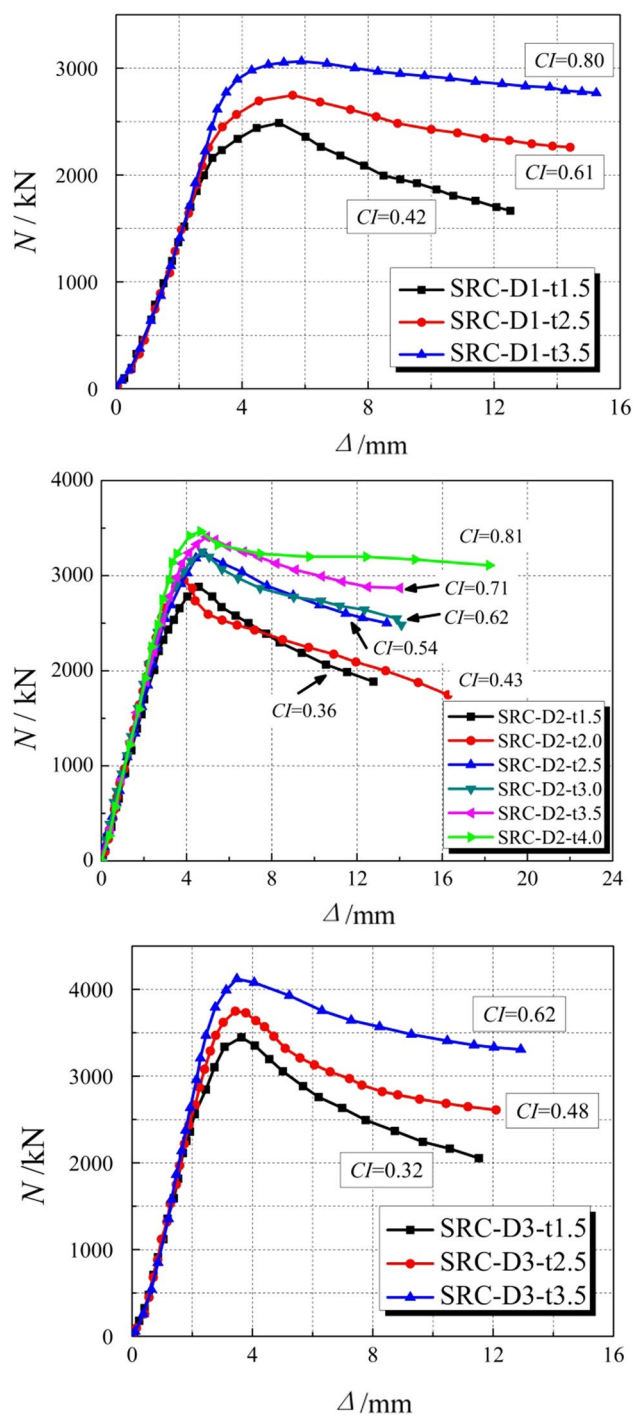

Fig. 10 Axial load-axial shortening curves with various confinement indexes

3.4 Strength Index

As we known, an important criterion to evaluate a strengthening method is the material strength utilization. In order to evaluate the material strength utilization, a strength index (*SI*) is defined for the SRC specimens as:

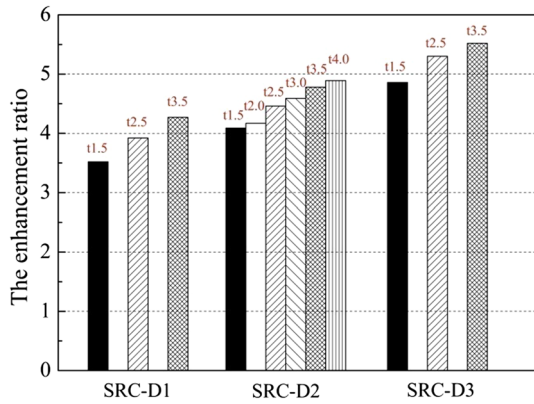$$SI = \frac{N_{\text{exp}}}{A_{c1}f_{c1} + A_{c2}f_{c2} + A_s f_{sy} + A_t f_{ty}} \tag{3}$$

Fig. 11 The values of enhancement ratio

Fig. 13 Comparisons of strength indexes in terms of the confinement index

where A_s and A_t are the cross-sectional areas of steel tube and longitudinal rebars, A_{c1} and A_{c2} are the cross-sectional areas of the original concrete and strengthening concrete, respectively. N_{exp} is the maximum load of the axial load-shortening curve of SRC columns. f_{sy} and f_{ty} are the yield strengths of the steel tube and longitudinal rebars, f_{c1} and f_{c2} are the axial compressive strengths of the original concrete and strengthening concrete, respectively.

Figure 12 shows the revolution of *SI* for strengthened columns in terms of the strengthened section diameter. Specimens SRC-D1-t1.5 and SRC-D2-t2.0 have the similar confinement index of 0.42. Specimens SRC-D1-t2.5, SRC-D2-t3.0 and SRC-D3-t3.5 have the similar confinement index of 0.62. Specimens SRC-D1-t3.5 and SRC-D2-t4.0 have the similar confinement index of 0.80. From Fig. 9, the specimen with larger strengthened section diameter has a smaller *SI*. Namely, with the similar confinement index, the material strength utilization drops as the strengthened section diameter increases.
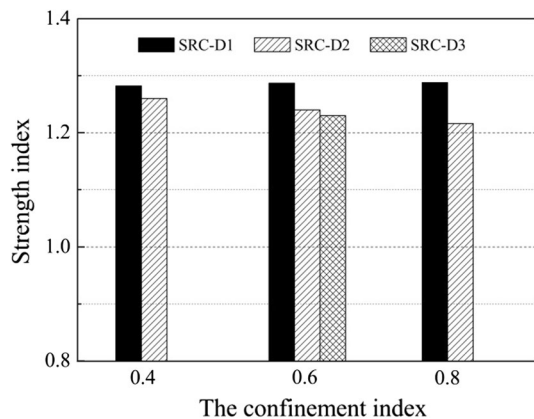
The effect of the confinement index (*CI*) on strength index (*SI*) is investigated in Fig. 13. For the series specimen SRC-D1, *SI* shows an increasing trend when the *CI* increases. For the series specimen SRC-D2 and SRC-D3, *SI* exhibits a decreasing trend with the increase of *CI*. It can be inferred that, with a small strengthened section diameter, the *SI* increases as the *CI* increases. When the strengthened section diameter goes beyond the limit, the *SI* drops with the increasing of *CI*. This can be attributed that when the strengthened section diameter is small, a higher *CI*-value represents a stronger confinement effect of steel tube. The confined concrete strength is higher due to tri-axial compression stress state. So the material utilization is more efficient. While the strengthened section diameter is large, the confinement effect is weak. A higher *CI* leads to the thicker steel tube. Due to the weak confinement effect, the thicker steel tube causes the lower material efficiency. Therefore, there is an optimum strengthened section diameter.

3.5 Ductility Index

To quantify the ductility of specimens more precisely, a ductility index is adopted in this study. Generally, the ductility index is defined as the ratio of the strain at $0.85\,N_u$ to the one at N_u. Due to the measurement deviation of strain, the ductility index is calculated by the axial load-shortening curves in this paper, and it can be given as:

$$DI = \frac{\Delta_{85}}{\Delta_u} \tag{4}$$

in which Δ_{85} is the average axial shortening when the applied load drops to $0.85\,N_u$, and Δ_u is the average axial shortening corresponding to N_u.

The calculated ductility indexes are listed in Table 1 and Fig. 14. As being shown that the *DI* of the RC columns is

Fig. 12 Comparisons of strength indexes in terms of the strengthened section diameter

(a)

(b)

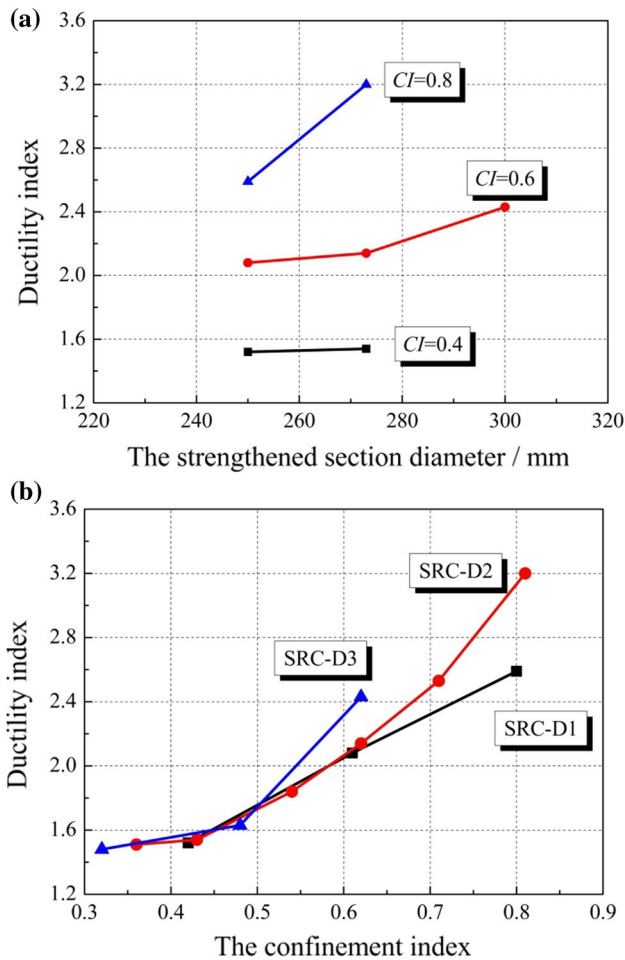**Fig. 14** Comparisons of the ductility index in terms of: **a** the strengthened section diameter, **b** the confinement index

significantly improved by the CFST strengthening method. The average improvement is about 48%. Figure 14a shows the trend line of *DI* in terms of the strengthened section diameter. With the similar level of *CI*, *DI* increases as the strengthened section diameter increasing. Figure 14b gives the comparisons of *DI*-value for the specimens with various confinement indexes. For the specimens with the same strengthened section diameter, *DI* increases with the increasing of the confinement index.

3.6 Relative Load-Strain Curve

The relative load-strain curves of all SRC columns are presented in Figs. 15, 16. The relative load is the ratio of the applied load (*N*) to the ultimate load (N_u). The strain is the average value of four strain gauges attached around the steel tube. All the relative load-strain curves have the same tendency. In the elastic stage, the curves approximately remain straight line, and the relative load has a significant linear correlation with the strain. When the load is up to
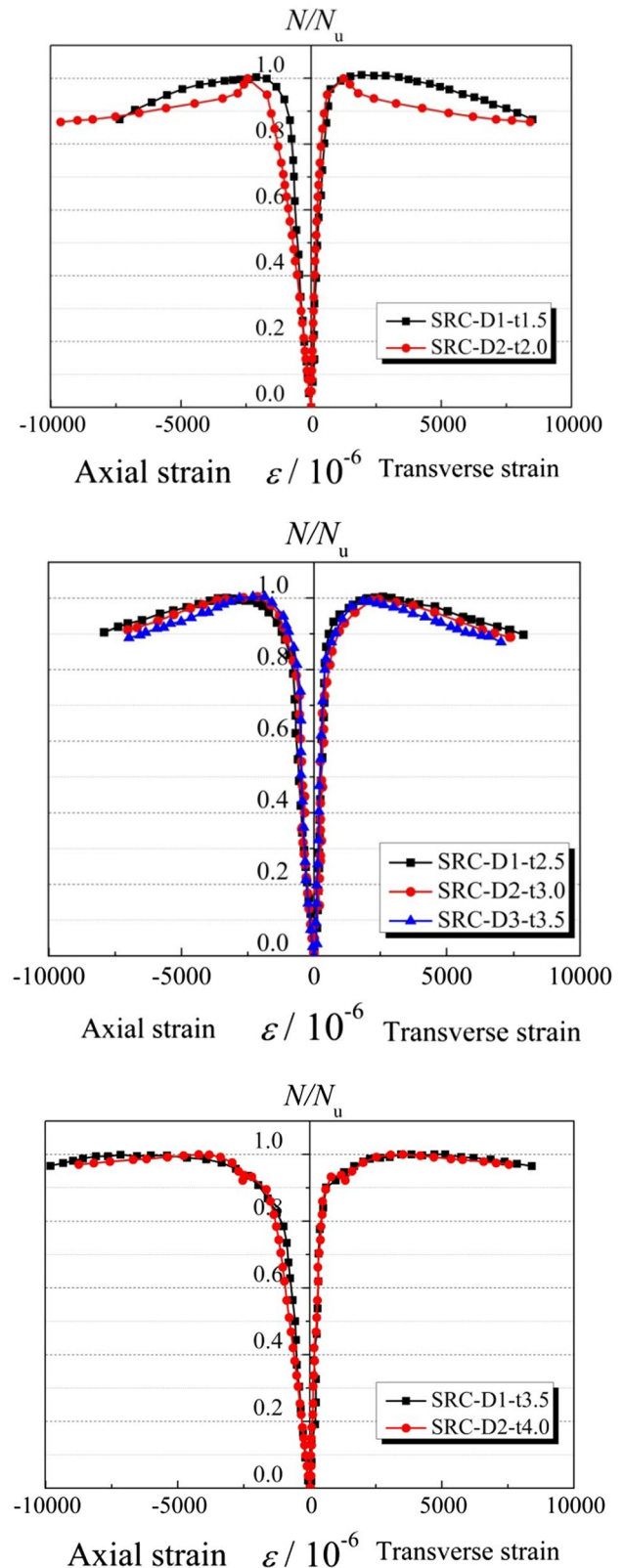

Fig. 15 Axial load-strain curves with various diameters of the strengthened section
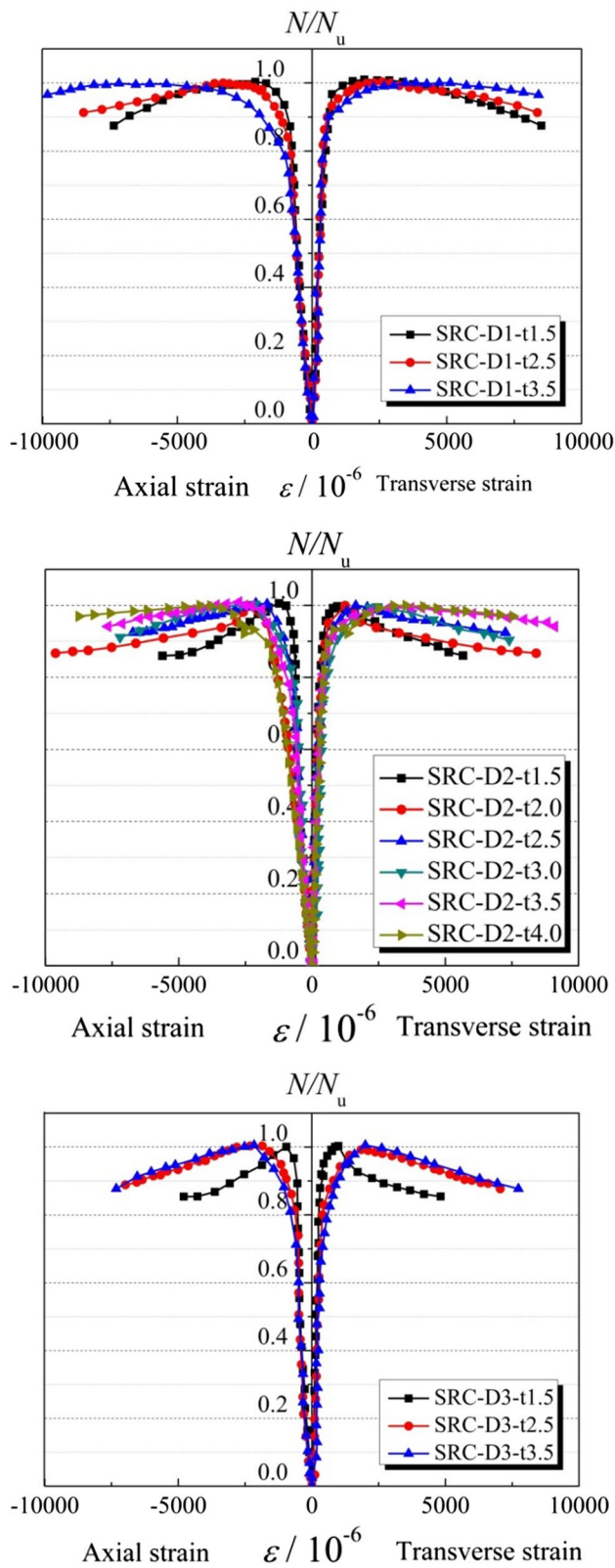
Fig. 16 Axial load-strain curves with various confinement indexes

80–85% of N_u, the curves begin to present elastic–plasticity. The growth of applied load reduces. After the peak load, the relative load drops gradually to about 85%.

Figure 15 shows the revolution of the relative load-strain curves in terms of the strengthened diameter. When the *CI*-value is same, the curves have no significant change in the elastic stage with the increase of strengthened diameter. The axial and transverse strains corresponding to the ultimate load almost remain unchanged. In the decline phase of the curves, the growth rate of the strains is higher as the strengthened diameter decreases.

Figure 16 compares the relative load-strain curves of the columns with different *CI*-values. The curves are almost coincided with each other in the elastic stage. Up to the ultimate load, the axial and transverse strains show an increasing trend as the *CI* increases. After the peak load, the growth rate of the strains increases with the higher *CI*.

3.7 Loading Distribution

To achieve loading distribution of SRC columns, the following assumptions are made:

1. The perfect bonding exists between concrete, reinforcement and steel tube so that no slippage can occur at the interface.
2. The radial stress of steel tube is neglected.
3. Reinforcements are under uniaxial tensile stress state.

   The total load (N_u) is shared by the components, so the equation of equilibrium can be given as:

$$N_u = N_c + N_s + N_t \tag{5}$$

in which N_c, N_s and N_t are the loads carried by concrete, steel tube and reinforcement, respectively.

They can be written in terms of stresses and the corresponding cross-sectional areas as following:

$$N_s = A_s \sigma_{sl} \tag{6}$$

$$N_t = A_t \sigma_{tl} \tag{7}$$

where σ_{sl} and σ_{tl} are the axial stresses of steel tube and reinforcement, respectively. Thus, σ_{sl} and σ_{tl} can be calculated by the constitutive relation of steel and the measured axial strains. When Eqs. (6) and (7) are subsisted into Eq. (5), the load carried by concrete (N_c) can be given.

The axial load-axial strain curves for concrete core, reinforcement and steel tube of the specimen SRC-D2-t2 are drawn separately in Fig. 17. It can be seen that in the initial stage, the carried load of each component is determined by its rigidity. As the load increases further, the bearing load proportion of concrete core gradually increases because of the confinement effect provided by the steel tube. The strain
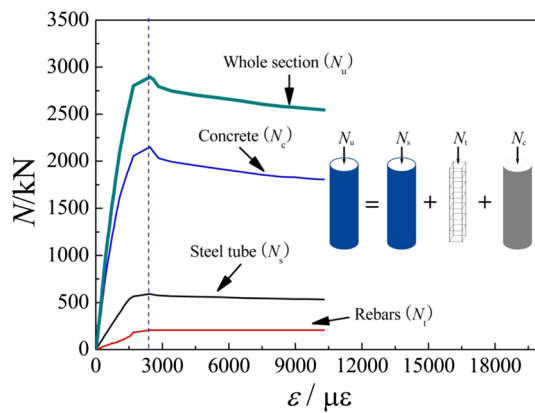
Fig. 17 Loading distribution of SRC-D2-t2

of concrete at maximum load N_c is larger than the yield strain of reinforcement and steel tube, namely the reinforcement and steel tube start to yield before the concrete reach to its maximum strength. It can be ascribed that the steel tube provides confining pressure to the concrete, which puts the concrete core under a tri-axial state of stress to improve its ultimate strength. After the yield strain of steel, the carried loads of each component keep constant at a certain level. The bearing load proportions of the components vary with the diameter of the strengthened section and the thickness of steel tube. The load proportion of concrete core is about 65–75%, the proportion of steel tube is about 15–25% and the proportion of the reinforcement is about 5%.

4 Conclusions

In this study, the test results of fourteen RC columns under axial load are conducted, including twelve columns strengthened with SCC filled circular steel tubes and the other two columns without strengthening as references. Based on the analysis above, the following conclusions are reached.

1. The CFST strengthening method has a significant impact on the ultimate capacity, rigidity and ductility. The average improvement of ultimate capacity is approximate 353%, and the mean increase of ductility index is about 50%, which indicating the effectiveness of this strengthening method.
2. With the same confinement index, a higher material strength utilization can be obtained with the smaller strengthened section diameter. The ductility of strengthened columns decreases with the increasing of strengthened section diameter.
3. There exists an optimum strengthed diameter to take full use of material strength. When the strengthened section

diameter is smaller than the optimum value, the material utilization shows an increasing trend with the increase of confinement index. As the strengthened section diameter exceed the optimum diameter, the material utilization drops with increasing confinement index.

References

Abdel-Hay, A. S., & Fawzy, Y. A. G. (2015). Behavior of partially defected R.C columns strengthened using steel jackets. *Housing and Building National Research Center Journal, 11,* 194–200.

Abedi, K., Afshin, H., & Shirazi, M. R. N. (2010). Numerical study on the seismic retrofitting of reinforced concrete columns using rectified steel jackets. *Asian Journal of Civil Engineering, 11*(2), 219–240.

Aboutaha, R. S., Engelhardt, M. D., Jirsa, J. O., & Kreger, M. E. (1999). Rehabilitation of shear critical concrete columns by use of rectangular steel jackets. *ACI Structural Journal, 96*(1), 68–78.

Bonacci, J. F., & Maalej, M. (2001). Behavioral trends of RC beams strengthened with externally bonded FRP. *Journal of Composites for Construction, 5*(2), 102–113.

Chitawadagi, M. V., Narasimhan, M. C., & Kulkarni, S. M. (2012). Axial strength of circular concrete-filled steel tube columns—DOE approach. *Journal of Constructional Steel Research, 66*(10), 1248–1260.

Colomb, F., Tobbi, H., Ferrier, E., & Hamelin, P. (2008). Seismic retrofit of reinforced concrete short columns by CFRP materials. *Composite Structures, 82*(4), 475–487.

Crawford, J. E., Malvar, L. J., Wesevich, J. W., Valancius, J., & Reynolds, A. D. (1997). Retrofit of reinforced concrete structures to resist blast effects. *ACI Structural Journal, 94*(4), 371–377.

Dundu, M. (2012). Compressive strength of circular concrete filled steel tube columns. *Thin-Walled Structures, 56,* 62–70.

Elremaily, A., & Azizinamini, A. (2002). Behavior and strength of circular concrete-filled tube columns. *Journal of Constructional Steel Research, 58*(12), 1567–1591.

GB 50367–2013. (2013). *Code for design of strengthening concrete structure*. Beijing: China Architecture and Building Press.

GBT 2975–1998. (1998). *Steel and steel products–location and preparation of test pieces for mechanical testing*. Bejing: China Standards Press.

Giakoumelis, G., & Lam, D. (2003). Axial capacity of circular concrete-filled tube columns. *Journal of Constructional Steel Research, 60*(7), 1049–1068.

Gilmour, J. R., & Virdi, K. S. (1988). Numerical modelling of the progressive collapse of framed structures as a result of impact or explosion. In *Proceedings of the second international Ph.D. Symposium in Civil Engineering*.

Gupta, P. K., Sarda, S. M., & Kumar, M. S. (2007). Experimental and computational study of concrete filled steel tubular columns under axial loads. *Journal of Constructional Steel Research, 63*(2), 182–193.

Han, L. H. (2007). *Concrete-filled steel tube columns*. Beijing: Science Press. **(in Chinese)**.

Han, L. H., Liu, W., & Yang, Y. F. (2008). Behaviour of concrete-filled steel tubular stub columns subjected to axially local compression. *Journal of Constructional Steel Research, 64*(4), 377–387.

Holschemacher, K. (2004). Hardened material properties of self-compacting concrete. *Journal of Civil Engineering and Management, 10*(4), 261–266.

Iqbal, S., Ali, A., Holschemacher, K., Bier, T. A., & Shah, A. A. (2016). Strengthening of RC beams using steel fiber reinforced high strength lightweight self-compacting concrete (SHLSCC) and their strength predictions. *Materials and Design, 100,* 37–46.

Kyung, J. S., Young, J. M., & Young, S. O. (2008). Seismic behaviour of composite concrete-filled tube column-to-beam moment connections. *Journal of Constructional Steel Research, 64,* 118–127.

Liu, H., Wang, Y. X., He, M. H., Shi, Y. J., & Waisman, H. (2015). Strength and ductility performance of concrete-filled steel tubular columns after long-term service loading. *Engineering Structures, 100,* 308–325.

Lu, Y. Y., Liang, H. J., Li, S., & Li, N. (2015a). Numerical and Experimental investigation on eccentric loading behavior of RC columns strengthened with SCC filled square steel tubes. *Advances in Structural Engineering, 18*(2), 295–309.

Lu, Y. Y., Liang, H. J., Li, S., & Li, N. (2015b). Axial behavior of RC columns strengthened with SCC filled square steel tubes. *Steel and Composite Structures, 18*(3), 623–639.

Lu, Y. Y., Liang, H. J., Li, S., & Li, N. (2015c). Eccentric strength and design of RC columns strengthened with SCC filled steel tubes. *Steel and Composite Structures, 18*(4), 833–852.

Muciaccia, G., Giussani, F., Rosati, G., & Mola, F. (2011). Response of self-compacting concrete filled tubes under eccentric compression. *Journal of Constructional Steel Research, 67*(5), 904–916.

Nanni, A., & Norris, M. S. (1995). FRP jacketed concrete under flexure and combined flexure-compression. *Construction and Building Materials, 9*(5), 273–281.

Patrick, P., Khayat, K. H., Daniel, C., & Stephan, T. (2005). Structural preformance of self-consolidating concrete used in confined concrete columns. *ACI Structural Journal, 102*(4), 560–568.

Pellegrino, C., & Modena, C. (2002). Fiber reinforced polymer shear strengthening of reinforced concrete beams with transverse steel reinforcement. *Journal of Composites for Construction, 6*(2), 104–111.

Priestley, M. J. N., Seible, F., Xiao, Y., & Verma, R. (1994a). Steel jacket retrofitting of reinforced concrete bridge columns for enhanced shear strength-part 1: Theoretical considerations and test design. *ACI Structural Journal, 91*(4), 394–405.

Priestley, M. J. N., Seible, F., Xiao, Y., & Verma, R. (1994b). Steel jacket retrofitting of reinforced concrete bridge columns for enhanced shear strength-part 2: Test results and comparison with theory. *ACI Structural Journal, 91*(5), 537–551.

Sezen, H., & Miller, E. A. (2011). Experimental evaluation of axial behavior of strengthened circular reinforced-concrete columns. *Journal of Bridge Engineering, ASCE, 16*(2), 238–247.

Sheikh, S. A., & Yau, G. (2002). Seismic behavior of concrete columns confined with steel and fiber reinforced polymers. *ACI Structural Journal, 99*(1), 72–80.

Uy, B., Tao, Z., & Han, L. H. (2011). Behaviour of short and slender concrete-filled stainless steel tubular columns. *Steel Construction, 67*(3), 360–378.

Vandoros, K. G., & Dritsos, S. E. (2008). Concrete jacket construction detail effectiveness when strengthening RC columns. *Construction and Building Materials, 22*(3), 264–276.

Wang, M. H. (2011). Experimental study on axial-compression reinforced concrete column strengthened by circular steel tube. *Applied Mechanics and Materials, 94–96,* 1261–1270.

Xiao, Y. (2003). Retrofit of reinforced concrete columns using partially stiffened steel jackets. *Journal of Structural Engineering, 129,* 725–732.

Xiong, M. X., Xiong, D. X., & Liew, J. Y. R. (2017). Axial performance of short concrete filled steel tubes with high- and ultra-high-strength materials. *Engineering Structures, 136,* 494–510.

Xu, J., & Cai, J. (2007). Research on the behaviour of reinforced concrete column strengthened by circular steel tube jacketing subjected to eccentric loading. *Industrial Construction, 37*(8), 14–17. **(in Chinese)**.

Yu, Z. W., Ding, F. X., & Cai, C. S. (2008). Experimental behavior of circular concrete-filled steel tube stub columns. *Steel Construction, 63*(2), 165–174.

Zhong, S. T. (2003). *The concrete-filled steel tubular structures*. China: Tsinghua University Press. **(in Chinese)**.

Zhou, M., Li, J. W., & Duan, J. M. (2012). Experimental study on the axial loading tests of RC columns strengthened with steel tube. *Applied Mechanics and Materials, 204–208,* 2878–2882.